Journal of Hazardous Materials 184 (2010) 567–573

Contents lists available at ScienceDirect

Journal of Hazardous Materials

journal homepage: www.elsevier.com/locate/jhazmat

Composition, diagenetic transformation and alkalinity potential of oil shale ash sediments

Riho Mõtlep [a,*], Terje Sild [b], Erik Puura [c], Kalle Kirsimäe [a]

[a] Department of Geology, University of Tartu, Ravila 14A, 50411 Tartu, Estonia
[b] Estonian Land Board, Mustamäe tee 51, 10621 Tallinn, Estonia
[c] Institute of Technology, University of Tartu, Nooruse 1, 50411 Tartu, Estonia

ARTICLE INFO

Article history:
Received 9 July 2010
Received in revised form 17 August 2010
Accepted 18 August 2010
Available online 26 August 2010

Keywords:
Oil shale ash
Mineralogy
Alkalinity
Ettringite

ABSTRACT

Oil shale is a primary fuel in the Estonian energy sector. After combustion 45–48% of the oil shale is left over as ash, producing about 5–7 Mt of ash, which is deposited on ash plateaus annually almost without any reuse. This study focuses on oil shale ash plateau sediment mineralogy, its hydration and diagenetic transformations, a study that has not been addressed. Oil shale ash wastes are considered as the biggest pollution sources in Estonia and thus determining the composition and properties of oil shale ash sediment are important to assess its environmental implications and also its possible reusability.

A study of fresh ash and drillcore samples from ash plateau sediment was conducted by X-ray diffractometry and scanning electron microscopy. The oil shale is highly calcareous, and the ash that remains after combustion is derived from the decomposition of carbonate minerals. It is rich in lime and anhydrite that are unstable phases under hydrous conditions. These processes and the diagenetic alteration of other phases determine the composition of the plateau sediment. Dominant phases in the ash are hydration and associated transformation products: calcite, ettringite, portlandite and hydrocalumite. The prevailing mineral phases (portlandite, ettringite) cause highly alkaline leachates, pH 12–13. Neutralization of these leachates under natural conditions, by rainwater leaching/neutralization and slow transformation (e.g. carbonation) of the aforementioned unstable phases into more stable forms, takes, at best, hundreds or even hundreds of thousands of years.

1. Introduction

Solid fossil fuels (e.g. coal) account for about one-quarter of the world's total primary energy supply, and their overall coal consumption is estimated to increase in coming decades due to the rising energy demand in fast-growing economies [1,2]. The combustion residues of used fuels thus pose an increasing threat to air quality, emission of greenhouse gases, and to soil and water quality. Moreover, growing demand forces employment of fossil fuels of lower quality like oil shale. The total world resources of oil shale (expressed as extractable shale oil) are at least 500 billion tonnes, whereas the mineral matter content of the commercial-grade oil shales varies between 77 and 87 wt% [3]. Large-scale exploitation of oil shale type fuel is operational only in Estonia, where kerogenous oil shale (8–12 MJ kg^{-1}) is used for oil retorting and for burning in electric Thermal Power Plants (TPP). The Estonian oil shale leaves after combustion large amounts of ash – 45 to 48 wt% of the raw oil shale. Reuse of the ash is limited and only a small proportion (less than 10%) of its production is used for construction materials (e.g. Portland cement, gas-concrete), in road construction (stabilization of roadbeds) and for agricultural purposes, e.g. liming of acid soils etc. [4]. Most of the ash is deposited in large waste plateaus next to the power plants. Approximately 280 million tonnes of ash has been disposed of since the 1950s, and at the current production level about 5–7 million tonnes of ash is added to the plateaus every year. Plateaus of deposited ash up to 45 m high at the two largest TPP-s, the Balti and the Eesti TPP, occupy about 20 km^2, and their area will grow until the oil shale is fired at Estonian TPP-s.

The oil shale is highly calcareous, and the ash remaining after combustion, derived from thermal decomposition of carbonate minerals, is rich in free lime (CaO) and anhydrite ($CaSO_4$). The ash removed from the boilers is transported to the plateaus through a pipe system as a water slurry at an ash–water ratio of 1:20. The unstable lime and anhydrite start to react with water already in ash removal system and the hydration processes continue in the open plateaus forming variety of secondary Ca-minerals. Due mainly to the formation of Ca-hydroxide (portlandite) and Ca–Al-sulphate (ettringite), the waters draining off the plateaus are of high alkalinity (pH 12–13). The highly alkaline leachates from the ash deposits

* Corresponding author. Tel.: +372 737 6689; fax: +372 737 5834.
E-mail addresses: riho.motlep@ut.ee (R. Mõtlep), terje.sild@maaamet.ee (T. Sild), erik.puura@ut.ee (E. Puura), kalle.kirsimae@ut.ee (K. Kirsimäe).

0304-3894/$ – see front matter © 2010 Elsevier B.V. All rights reserved.
doi:10.1016/j.jhazmat.2010.08.073

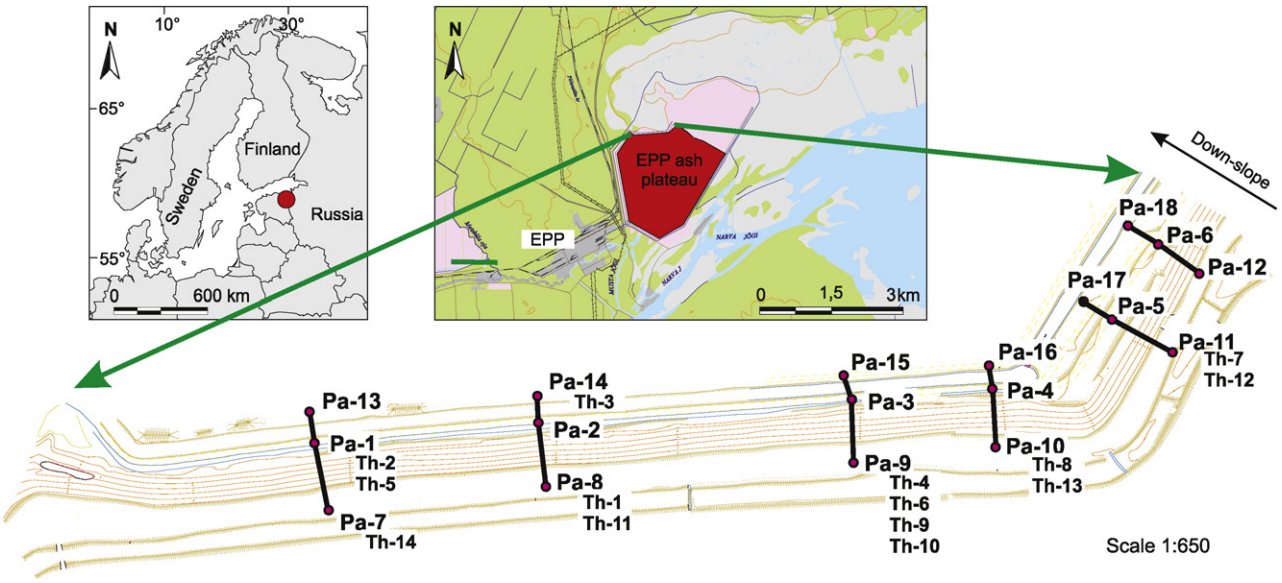

Fig. 1. Location of the ash plateau and a settings of studied drillhole samples. Pa – drillhole no., Th – sample no.

pose an environmental risk, and the ash plateaus are considered as major pollution sources [5]. The alkalinity potential of ash waste depends directly on the mineral composition and diagenetic evolution of the sediment. However, under atmospheric conditions, portlandite and ettringite are metastable phases and evolve into environmentally stable minerals – calcite/aragonite and gypsum.

The composition and transformation of oil shale ash with hydration has been studied since the 1950s [6–12]. However, the mineral and geochemical transformation of the ash plateau sediments has not yet been addressed. In this contribution we study the quantitative mineralogy of the oil shale ash plateau sediment, its diagenetic transformation and alkalinity potential. These results are important for understanding and estimating the potential environmental threats of the deposited ash materials.

2. Materials and methods

The material investigated was sampled from the ash plateau deposits at the Eesti TPP. Drillcore samples were obtained from geotechnical drilling in the northern part of the plateau, with a maximum depth of 33.7 m from the top of the plateau. The drillcores were made by partial coring only, and the samples from the different drillcore profiles were used to produce a composite depth profile. Altogether 14 samples from 7 drillcores were investigated (Fig. 1). In addition to the core samples, 6 samples of fresh ash fractions (fly-ash and bottom/slag ash) from the pulverized firing furnace of the Eesti TPP were investigated for mineralogical composition. Only the pulverized firing (PF) ash was selected because circulating fluidized bed (CFB) firing was introduced at the Eesti TPP in 2004, and most of the plateau deposits are composed of PF ashes. The composition and hydration of fluidized bed firing ash are discussed by Kuusik et al. [11] and Liira et al. [12].

The mineralogical composition of the samples was studied by means of powder X-ray diffraction. Randomly oriented powders were measured on a Dron 3M diffractometer using Ni-filtered Cu Kα radiation over the 2–50° 2θ region, with a scan step of 0.02° 2θ and a count time of 5 s per step, and on a Bruker D8 diffractometer using Ni-filtered Cu Kα radiation over 2–70° 2θ region, with a scan step of 0.02° 2θ and a count time of 2 s per step. Quantitative mineral composition was determined by full-profile Rietveld analysis using the Siroquant™ software system [13,14]. The portion of non-diffracting amorphous (glass-like) phase(s) was estimated from its mass-adsorption effect on the pattern with an added spike of a known phase (halite – NaCl). A mass-adsorption coefficient of silicate composition glass was assumed for the amorphous phases. The accuracy of the amorphous phase determination is not better than 20%.

Micromorphology of ash sediment samples was studied using a Zeiss DSM 940 scanning electron microscope (SEM), equipped with an Idfix Si-drift technology energy-dispersive analyzer (EDS). SEM preparations were coated with conductive gold or carbon during preparation.

Alkalinity potential of the oil shale ash sediment was calculated according to the empirical function presented by [24,25]:

$$\mathrm{ALK} = 97(\mathrm{Ca_{NS}}) + 175 \quad (1)$$

where ALK – alkalinity, meq NaOH g^{-1}; Ca_{NS} – non-silicate calcium, meq g^{-1}.

The neutralization volume of the plateau sediments as a function of Ca was found according to [25]:

$$V_N = \frac{(0.032\mathrm{Ca} - 0.09)}{N} \quad (2)$$

where V_N – neutralization volume, L kg^{-1}; Ca – Ca concentration, g kg^{-1}; N – normality of the acid, eq L^{-1}.

3. Results

Characteristic X-ray patterns and the mineralogical composition of the samples are shown in Figs. 2–6, and Tables 1 and 2. The micromorphology of the unhydrated and hydrated ash samples is shown in Fig. 7.

3.1. Fresh ash

The composition of the fresh unhydrated ash fractions at the Eesti TPP is dominated by free lime (CaO), anhydrite ($CaSO_4$), C2S/belite (β-Ca_2SiO_4) quartz (SiO_2), calcite ($CaCO_3$) and K-feldspar. The ash contains also lesser proportions of periclase (MgO), melilite ($(Ca,Na)_2(Mg,Al)(Si,Al)_3O_7$), merwinite – $Ca_3Mg(SiO_4)_2$, (pseudo)wollastonite ($CaO{\cdot}SiO_2$), hematite (Fe_2O_3), brownmillerite ($Ca_2(Al,Fe^{3+})_2O_5$) and C3A (calcium aluminate), with few traces of a secondary hydration product – portlandite – $Ca(OH)_2$ (Fig. 2; Table 1). The mineral composition as well as the

Table 1
Mineral composition of fresh unhydrated ash samples. Furnace, economizer, cyclone, EP1, 2, 3 (electrostatic precipitation filters 1, 2, 3, respectively) are listed in the table respect to their positions in boiler technological scheme.

	Amorphous phase (%)	Quartz (%)	Lime (%)	Portlandite (%)	Calcite (%)	Anhydrite (%)	Melilite (%)	Periclase (%)	Belite (C2S) (%)	Merwinite (%)	Wollastonite (%)	K-feldspar (%)	Hematite (%)	C3A (%)	Brownmillerite (%)	Sylvite (%)
Furnace	27.3	4.4	23.5	tr.[a]	12.3	3.4	5.6	3.4	8.3	0.9	2.3	3.3	tr.	2.1	1.9	tr.
Economizer	36.5	3.7	16.0	1.7	4.9	6.0	5.7	2.9	9.8	2.3	2.6	3.2	tr.	2.0	1.9	tr.
Cyclone	37.8	3.7	18.9	tr.	3.4	4.8	3.9	2.8	11.2	2.4	2.5	3.0	tr.	2.0	2.3	tr.
EP1[b]	28.3	6.1	8.3	tr.	4.5	14.4	4.0	2.1	10.0	tr.	5.8	8.2	1.7	2.5	2.0	1.5
EP2	22.6	7.9	12.8	tr.	5.1	14.3	3.6	2.6	10.8	tr.	5.2	6.9	1.6	2.9	1.7	1.1
EP3	1.1	10.4	20.0	tr.	6.7	15.4	4.2	3.5	15.2	1.2	5.1	7.5	1.7	3.4	3.4	1.2

[a] tr. – trace.
[b] EP 1, 2, 3 – electrostatic precipitator nos. 1, 2, 3, respectively.

Table 2
Mineral composition (including amorphous phase) of hydrated ash sediments from the EPP ash plateau.

Sample	Depth (m)	Average depth (m)	Amorphous phase (%)	Quartz (%)	K-feldspar (%)	Smectite (%)	Calcite (%)	Portlandite (%)	Ettringite (%)	Hydrocalumite (%)	Belite (C2S) (%)	Gypsum (%)	Melilite (%)	Vaterite (%)	Lime (%)
th-01	0.4–0.6	0.5	5.7	7.3	4.9	4.5	41.0	8.4	14.6	13.5					tr.
th-02	2.3–2.35	2.32	9.1	4.6	2.3	5.9	35.1		21.4	14.9	5.2		1.6		
th-03	2.5–2.7	2.6		4.3	3.4	3.1	30.7	10.0	27.9	7.7	8.3	tr.[a]	3.9		
th-04	3.0–3.2	3.1	4.8	8.2	10.5	1.9	25.1		26.2	10.1	9.2		4.0		
th-05	3.25–3.30	3.27	17.4	4.5	4.9	2.4	27.5	tr.	24.0	7.7	6.8			4.3	
th-06	3.4–3.8	3.6		9.6		5.3	15.0	4.9	31.0	22.8	11.3				
th-07	9.0–9.3	9.15	11.6	5.8	3.0	3.3	14.8	8.2	24.4	16.0	6.4	1.3	3.3	2.0	
th-08	10.2–10.7	10.45	1.7	5.9	6.0	2.8	26.3	1.5	25.5	10.6	9.5		3.2	7.0	
th-09	12.0–12.4	12.2	tr.	6.1	7.2	2.7	21.0	8.2	23.1	17.2	7.6	2.4	4.3		
th-10	14.1–14.2	14.15	26.0	2.2	6.4	1.0	13.3	10.5	6.4	13.5	7.5	3.3	9.9		
th-11	22.4–22.6	22.5	40.1	5.4	10.9	1.5	15.8	2.5	3.0	6.2	9.0		5.7		
th-12	22.8–23.3	23.05	tr.	2.2	3.7	2.5	24.6	16.6	17.8	12.7	9.9		7.3	2.5	
th-13	24.0–24.3	24.15	23.8	4.4	6.8	3.6	13.2	1.5	23.5	7.9	9.1		4.1	2.0	
th-14	26.0–26.35	26.17	36.5	3.0	3.1	1.4	16.6	tr.	25.4	4.8	5.4		1.1	2.0	

[a] tr. – trace.

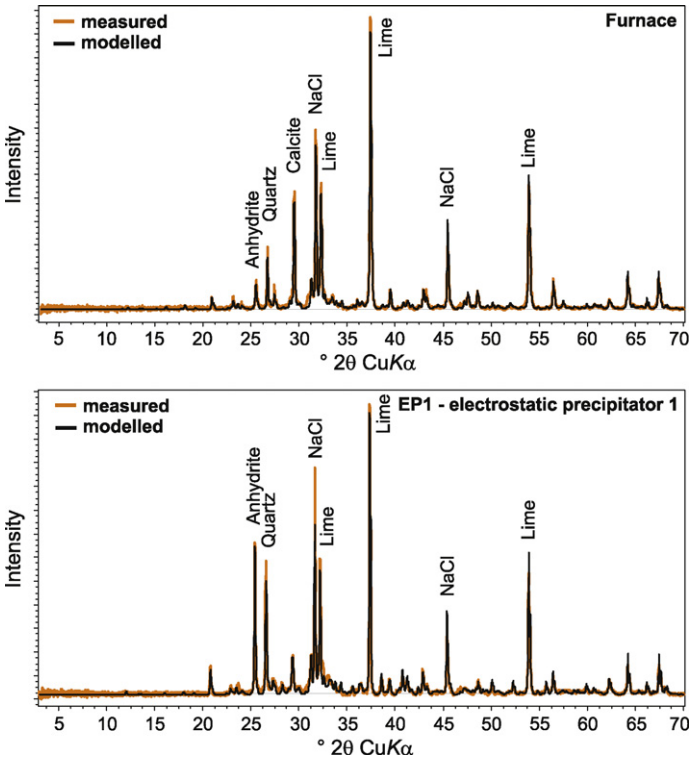

Fig. 2. Representative XRD patterns of the fresh unhydrated ash from furnace (upper) and cyclone. Figures represent measured (red) and modelled (black) traces, dominant phases are indicated next to their highest reflexes. (For interpretation of the references to color in this figure legend, the reader is referred to the web version of the article.)

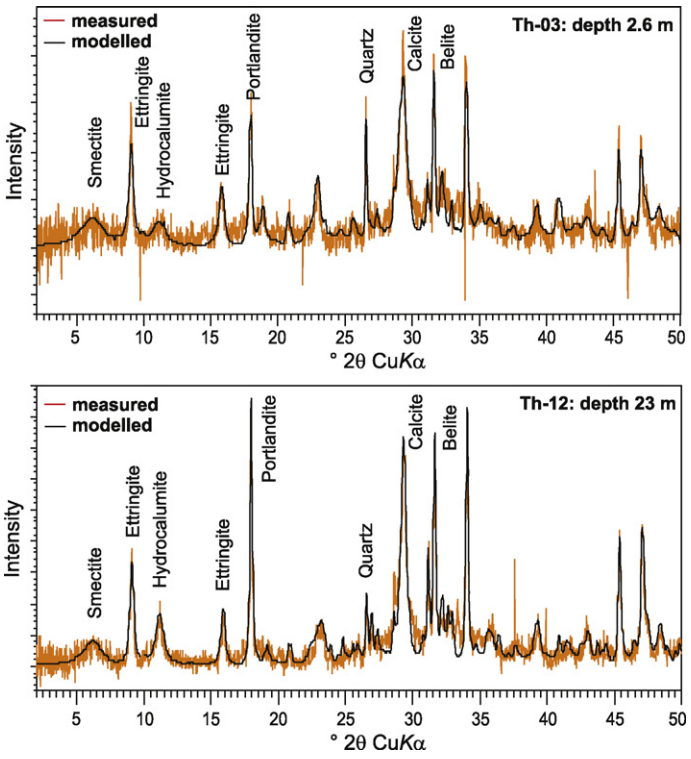

Fig. 4. Representative XRD patterns (samples th-03 and th-12) of the ash plateau sediments from different locations and depth.

average grain size of the unhydrated ash fractions varies systematically with the position in the ash removal system (Fig. 3). The average grain size of ash fractions decreases along the boiler gas pass, being coarsest in furnace ash (~250 μm) and finest in the last field of electrostatic precipitators (~6 μm). The proportion of lime as a dominant phase in the fresh ash decreases in the first half of the ash removal system but, surprisingly, at the electrostatic precipitators the lime content increases from 8% to 20%. Similar trends apply to variations in the periclase content, and also somewhat to melilite. Anhydrite, on the other hand, as well as thermally resistant

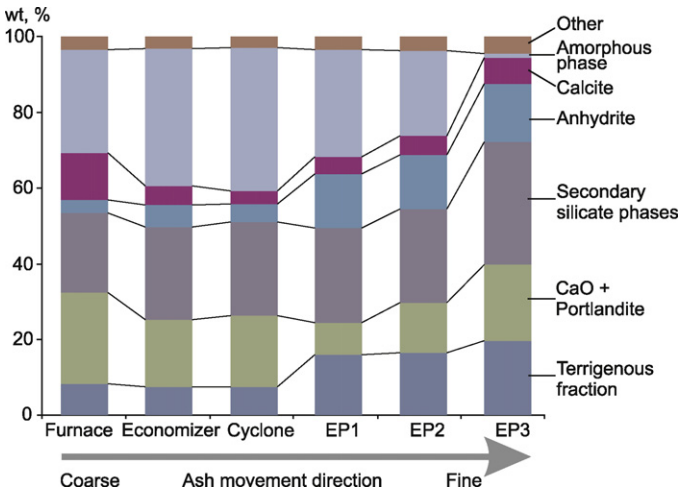

Fig. 3. The quantity of different mineral phases in the fresh unhydrated oil shale ash. "Terrigenous fraction" sum of quartz, K-feldspar and hematite; "secondary silicate phases" sum of belite, merwinite, melilite, wollastonite, calcium aluminate and brownmillerite; "others" include minor phases like periclase and sylvite.

quartz and K-feldspar, increases monotonously with the decreasing particle size in the different ash filter systems; these phases reach about 15%, 10% and 7.5%, respectively, in the final stage of the electrostatic filters (Fig. 3).

The proportion of amorphous phase behaves in an opposite way to lime. The samples show an increasing trend for amorphous phase from furnace to cyclone; however, further along the boiler gas pass, the amorphous content starts to decline, dropping from almost 38% down to 1%.

3.2. Plateau sediments

The composition of the plateau sediments is highly variable (Fig. 4; Table 2). The main mineral phases are calcite, ettringite – $Ca_6Al_2(SO_4)_3(OH)_{12}{\cdot}26H_2O$, portlandite, hydrocalumite – $Ca_2Al(OH)_7{\cdot}3H_2O$, C2S/belite, merwinite and melilite, with quartz and orthoclase type K-feldspar. Gypsum, vaterite and authigenic smectite are typical minor phases (Table 2).

The proportion of calcite varies from 40% in the shallow depth samples and in the surface layer of the deposit to about 15% in the deepest samples (Fig. 5). In contrast, the proportion of portlandite (on average 5.2%) is lower in shallow buried samples, but reaches up to 16% in sample th-12 at 23 m depth. The proportion of ettringite ranges between 15% and 30%, except in samples th-10 and th-11, where the ettringite content is only about 6% and 3%, respectively. The proportions of hydrocalumite, belite and melilite vary without noticeable trend from 5% to 23%, 5% to 11% and 1% to 10%, respectively (Table 2; Fig. 5).

The proportions of thermally resistant phases, quartz and K-feldspar, is rather stable in all samples studied, and varying between 2–10% and 2–11%, respectively. The ratio of quartz to K-feldspar in hydrated ash sediment corresponds approximately to the ratio of these minerals in the raw oil shale. Small amounts of smectite were also detected, the content of which was highest in the uppermost samples (up to 6%). The proportion of amorphous

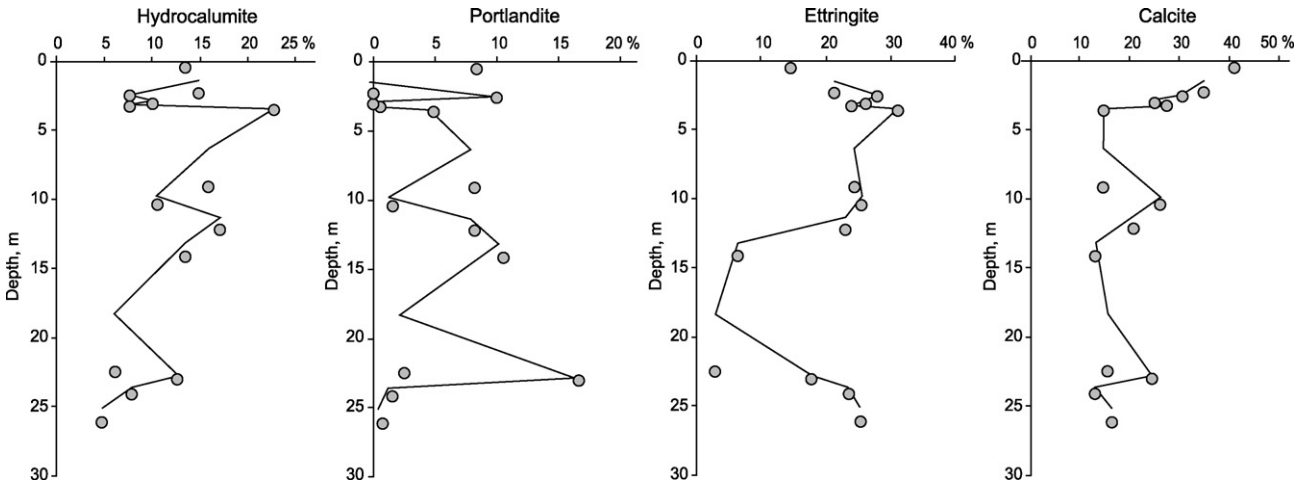

Fig. 5. The depth profiles of dominant phases: ettringite, portlandite, calcite and hydrocalumite in the ash plateau sediments. The continuous line represents 2 period moving average.

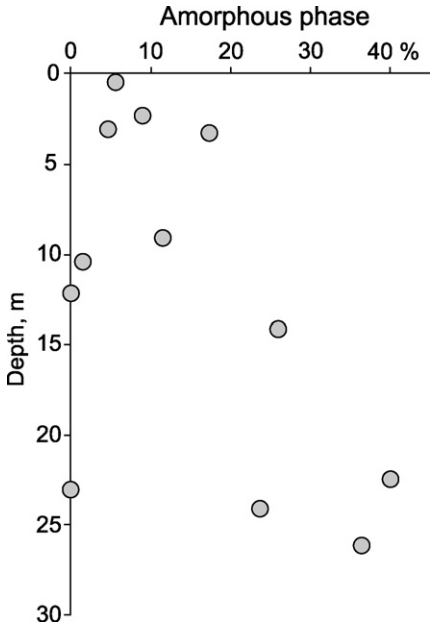

Fig. 6. Variations of amorphous phase with depth.

phase increases from about 6% in shallow depth samples to up to 40% in sample th-11 at a depth of 22.5 m. However, the amount of amorphous phase in the samples studied shows a considerable variation (Table 2; Fig. 6).

The microstructure of the hydrated ash contains abundant plates of portlandite, needle-like prismatic ettringite crystallites (which form irregular and/or spherulitic aggregates in the pore space), and altered spherulitic glass aggregates (Fig. 7). The surface samples also contain secondary calcium carbonate precipitates, which occur in the form of euhedral crystallite aggregates (Fig. 7D).

4. Discussion

According to Ots [4] the proportions of the different ash fractions in averaged ash flow is 39.3% bottom-slag ash; 3.1% superheater ash; 4.7% economizer ash; 32.2% cyclone ash and 13.5%, 3.1%, 0.7% of electrostatic precipitators 1, 2 and 3, respectively. This suggests that the average composition of the ash deposited on the ash plateaus is dominated by free lime (17%), anhydrite (10%) and belite (11%). First two mineral phases are unstable under hydrous conditions and are rapidly hydrated/transformed into metastable hydrous phases. The first reaction of raw ash hydration is lime slacking that leads to formation of portlandite (3).

$$CaO + H_2O \rightarrow Ca(OH)_2 \quad (3)$$

The experimental hydration of oil shale PF and CFB ashes [11,12] suggests that the lime to portlandite conversion is fast, and almost complete lime slaking occurs during the first 24 h of reaction. The next stage of the oil shale ash hydration is governed by anhydrite (anhydrous Ca-sulphate) reactions towards gypsum (4) and ettringite (5).

$$CaSO_4 + 2H_2O \rightarrow CaSO_4{\cdot}2H_2O \quad (4)$$

$$3Ca(OH)_2 + 2Al(OH)_3 + 3CaSO_4 + 26H_2O \rightarrow Ca_6Al_2(SO_4)_3(OH)_{12}{\cdot}26H_2O \quad (5)$$

Ettringite forms from reaction of the anhydrite/gypsum and dehydroxylated aluminosilicate clays and/or amorphous Al–Si glasses. Liira et al. [12] shows that ettringite was detected by X-ray diffraction in oil shale ash after about 5–14 days, when free lime was converted to portlandite and the cabonation of portlandite had already been started. This does not agree with earlier studies [15] suggesting that ettringite forms during early stages of hydration. The phenomenon of delayed ettringite occurrence can be explained either by an early colloidal (X-ray amorphous) form of the ettringite that cannot be detected by X-ray diffraction [e.g. 16] or by inhibited precipitation of the ettringite due to limited diffusion of the $Al(OH)_4^-$ ions into the pore solution in the presence of gypsum and lime, where lime depresses the solubility of the potential aluminium bearing phases – aluminate, aluminosilicate glass, clay minerals and K-feldspar [17]. The latter suggests that the aluminium becomes available for ettringite formation after the slaking of the lime is completed, which agrees with the observed timing of the ettringite formation.

The formation of hydrocalumite ($Ca_2Al(OH)_7{\cdot}3H_2O$) as the next secondary phase in PF ash hydration process suggests that the ettringite formation in oil shale ashes is limited by the availability of dissolved sulphate, while the excess of aluminium is precipitated as Ca-aluminate(hydrate) type phases. However, Liira et al. [12] noted that in CFB ashes ettringite formation is accompanied by precipitation of excess gypsum ($CaSO_4{\cdot}2H_2O$), which implies that aluminium, not sulphate, is a limiting component in these ashes.

Subsequent diagenetic transformation of the hydrated ash is governed by carbonation of the metastable portlandite by binding

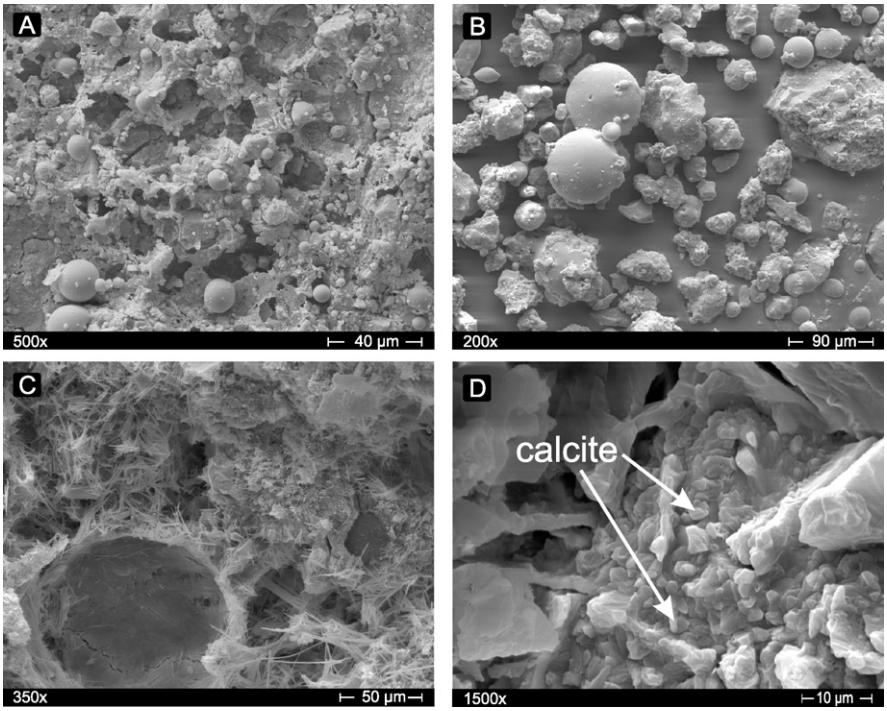

Fig. 7. SEM images of unhydrated (A and B) and the plateau sediment samples (C and D). Fresh ash from furnace (A) and from cyclone (B) show abundant spherulitic glass aggregates. (C) Abundant needle-like ettringite crystallite fillings in sediment voids and a remnant form of spherulitic glass aggregate with ettringite coating. (D) Secondary calcium carbonate precipitates on the surface sample sediments.

of atmospheric CO_2 according to reaction (6).

$$Ca(OH)_2 + CO_2 \rightarrow CaCO_3 + H_2O \quad (6)$$

As a result the composition of the ash stored under ambient conditions is progressively modified [9,12,18,19]. According to Kuusik et al. [10] complete carbonation of portlandite in laboratory scale experiments takes place in 28 days. Our results show, however, that significant (but not complete) carbonation of portlandite is achieved only in the uppermost 0.5–1 m thick layer of the ash plateau sediments, and the content of calcite decreases over (through) about a 5 m thick depth interval, whereas the portlandite is well preserved in deeper parts of the ash plateau sequence. This observation suggests slow CO_2 diffusion controlled carbonation of the plateau sediments, which is further retarded in the upper layers of the ash deposits due to the effective precipitation of calcite and other secondary minerals that will progressively block out the pore space.

Slow carbonation of the ash sediment is important in retaining stability of other primary hydration phases, especially ettringite. Ettringite stability is controlled by pH and sulphate activity, and the phase is stable at pH values >10.7 [20]. At lower pH values the ettringite becomes unstable and dissolves incongruently to gypsum/bassanite, (amorphous) Al-hydroxide and Ca-aluminate type phases (reaction 7) [20], or in the presence of CO_2 to Ca-sulphate, Al-gel and calcium carbonate (aragonite, vaterite, calcite) [21].

$$Ca_6Al_2(SO_4)_3(OH)_{12}{\cdot}26H_2O + 3CO_2 \rightarrow 3CaCO_3 + 2Al(OH)_3 + 3CaSO_4{\cdot}0.5H_2O + 27.5H_2O \quad (7)$$

Portlandite dissolution equilibrium controls the solution pH at pH ~ 12.3, which is well above the ettringite stability limit, and in deeper parts of the ash plateau the ettringite is a stable phase. However, the calcite equilibrium (pH ~ 8.2) is attained by carbonation of the portlandite in the system and ettringite becomes unstable. This process is evident only in the uppermost layer of the plateau sediments, where the proportion of ettringite has somewhat decreased, but in the presence of some amounts of portlandite the pH is still at the ettringite stability level (pH ~ 12).

Diagenetic transformation of the secondary Ca-silicate phases formed in the burning processes is subdued, although belite (β-$CaSiO_4$) can react with atmospheric CO_2 forming additional $CaCO_3$ – calcite and SiO_2 – quartz (reaction 8) [10].

$$Ca_2SiO_4 + 2CO_2 = 2CaCO_3 + SiO_2 \quad (8)$$

The composition trends of the Ca-silicate phases in the plateau sediments (Table 2) does not show any changes, and the transformation of silicate mineral phases can be regarded as a minor. Nevertheless, the mineralogical data suggest dissolution of amorphous glass phases and precipitation of secondary smectite type clay phases. Higher proportions of clay and decreasing proportions of amorphous phase in the uppermost part of the deposit suggest a dissolution–precipitation mechanism of glass devitrification, which is most probably initiated by percolating unsaturated precipitation waters. The recrystallization of the glass phases is also indicated by dissolution pits, as well as secondary coatings on the surfaces of spherulitic glass particles (Fig. 7C). High activity of dissolved Si and specifically high K (>500 mg l^{-1}) [22] in the water in contact with the ash would hint at the precipitation of secondary mixed-layer clays, zeolites and/or authigenic K-feldspar phases similar to hydration of volcanic glasses in evaporitic alkaline hypersaline or diagenetic environments [e.g. 23]. However, secondary silicates other than smectite type clay were not identified in the ash plateau sediments.

4.1. Alkalinity potential

High alkalinity (pH 12–13) of the waters draining off from the ash sediment plateaus is controlled by the content of portlandite and ettringite, which are the main secondary Ca-hydrate phases in the plateau sediments. Our results show that stabilization of the plateau sediments by carbonation and precipitation of stable calcite has affected only a limited volume of surface sediments,

meaning that the sediment heaps retain a high alkalinity potential for a long time. Alkalinity (potential) or buffering capacity of the ash sediments can be estimated as a function of the concentrations of alkaline elements and cations of strong bases (Ca, Mg and Na, K, respectively) [24,25], whereas the non-silicate Ca concentration has been found to yield a linear empirical function with the alkalinity for different types of fly ashes [Eq. (1), 25]. Based on this we can define the neutralization volume (i.e. volume of acid required to neutralize a mass unit of alkaline ash sediment) of the plateau sediments as a function of Ca [Eq. (2), 25].

According to the mineralogical analyses (Table 2) the proportion of non-silicate Ca in the ash plateau sediments varies from 18% to 32%, average 25%. The corresponding average estimated alkalinity of the ash sediment is thus 1195 $meq_{NaOH}\ g^{-1}$. Under open conditions the neutralization of the ash alkalinity occurs by slightly acidic (pH 5.65) natural precipitation. The precipitation water in equilibrium with atmospheric CO_2 contains 9.3×10^{-6} mol L^{-1} of carbonic acid, which suggests that about 7×10^5 L of rain water is required for full neutralization (pH 7) of 1 kg of ash sediment. The mean annual amount of precipitation in Estonia is about 760 mm $year^{-1}$ and the density of the ash sediment varies between 1800 and 2500 kg m^{-3} (average 2100 kg m^{-3}). Under these circumstances the neutralization of one cubic metre of ash sediment would require a percolating rainwater volume equivalent to the precipitation in about 400 thousand years. Recently Velts et al. [26] estimated using numerical modelling of Ca leaching from a 1 m thick layer of oil shale ash that leaching of soluble part of the lime with natural precipitation would take approximately 500 years. Although this model does not take into account the diagenetic transformation of the unstable ash minerals it is evident that hydrated oil shale ash sediments maintain high alkalinity and alkaline pH for considerably long times, posing a potential environmental threat for coming centuries. More explicit estimates of the time and conditions required to neutralize fluid in a waste deposit fill would need further research to understand the rates of water infiltration and diffusion of CO_2, as well as anion hydrolysis of the silicate phases.

5. Conclusions

Ash left after burning kerogenous Estonian oil shale is composed of lime, anhydrite, Ca-silicate mineral phases, and X-ray amorphous Al–Si glass phase, which are unstable under open atmospheric and wet conditions, and become hydrated into metastable secondary phases portlandite (calcite), gypsum, ettringite and hydrocalumite. Diagenetic transformation of the hydrated ash is dominated by carbonation of metastable portlandite by reaction with atmospheric CO_2. Slow carbonation allows preservation of primary hydration phases, such as ettringite. Ettringite and portlandite dissolution maintain the solution pH at 12–13. Alkalinity potential estimated from the composition of the ash shows that the full neutralization of ash sediment by precipitation water would require hundreds of thousands of years, making these ash plateaus environmental problems for many coming generations.

Acknowledgements

This research was funded by Estonian Target Financed Research Project SF0180069s08. Three anonymous reviewers are acknowledged for critical reading of the manuscript.

References

[1] IEA, World Energy Outlook, International Energy Agency, Paris, 2006.
[2] A. Dellantonio, W.J. Fitz, F. Repmann, W.W. Wenzel, Disposal of coal combustion residues in terrestrial systems: contamination and risk management, J. Environ. Qual. 39 (2010) 761–775.
[3] V. Puura, E. Puura, Origins, compositions, and technological and environmental problems of utilization of oil shales, Estonian J. Earth Sci. 56 (2007) 185–187.
[4] A. Ots, Oil Shale Fuel Combustion, Tallinna Raamatutrükikoda, Tallinn, 2006.
[5] L. Savitskaja, Man-made changes of groundwater quality, in: A. Raukas, A. Teedumäe (Eds.), Geology and Mineral Resources of Estonia, Estonian Academy Publishers, Tallinn, 1997, pp. 152–156.
[6] G. Mets, V. Kikas, The use of the methods of X-raying for the study of the mineralogical composition of oil shale ash, Oil Shale Ash Build. (1955) 89–94 (in Russian).
[7] N. Dilaktorski, Theoretical basis for the utilization of the mineral compounds of oil shale in building industry, Stud. Build. 3 (1962) 5–45 (in Russian, summary in English).
[8] L. Pets, Probable modes of occurrence of trace elements in oil shale ashes of power plant, Oil Shale 16 (1999) 464–472 (in Russian).
[9] A. Paat, R. Traksmaa, Investigation of the mineral composition of Estonian oil shale ash using X-ray diffractometry, Oil Shale 19 (2002) 373–386.
[10] R. Kuusik, A. Paat, H. Veskimäe, M. Uibu, Transformations in oil shale ash at wet deposition, Oil Shale 21 (2004) 27–42.
[11] R. Kuusik, M. Uibu, K. Kirsimäe, Characterization of oil shale ashes formed at industrial-scale CFBC boilers, Oil Shale 22 (2005) 407–421.
[12] M. Liira, K. Kirsimäe, R. Kuusik, R. Mõtlep, Transformation of calcareous oil-shale circulating fluidized-bed combustion boiler ashes under wet conditions, Fuel 88 (2009) 712–718.
[13] J.C. Taylor, Computer programs for standardless quantitative analysis of minerals using the full powder diffraction profile, Powder Diffr. 6 (1991) 2–9.
[14] C.R. Ward, C.J. Taylor, D.R. Cohen, Quantitative mineralogy of sandstones by X-ray diffractometry and normative analysis, J. Sed. Geo. 69 (1999) 1050–1062.
[15] H.F.W. Taylor, Cement Chemistry, second ed., Thomas Telford, London, 1997.
[16] P.K. Mehta, Effect of lime on hydration of pastes containing gypsum and calcium aluminates or calcium sulfoaluminate, J. Am. Ceram. Soc. 56 (1973) 315–319.
[17] M. Deng, M. Tang, Formation and expansion of ettringite crystals, Cement Concrete Res. 24 (1994) 119–126.
[18] R. Kuusik, H. Veskimäe, M. Uibu, Carbon dioxide binding in the heterogeneous systems formed at combustion of oil shale – 3. Transformations in the system suspensions of ash–flue gases, Oil Shale 19 (2002) 277–288.
[19] T. Kaljuvee, R. Kuusik, M. Radin, V. Bender, Carbon dioxide in the heterogeneous systems formed at combustion of oil shale – 4. Reactivity of ashes towards acid gases in the system fly ash–flue gases, Oil Shale 21 (2004) 13–26.
[20] S.C.B. Myneni, S.J. Traina, T.J. Logan, Ettringite solubility and geochemistry of the $Ca(OH)_2$–$Al_2(SO_4)_3$–H_2O system at 1 atm pressure and 298 K, Chem. Geol. 148 (1998) 1–19.
[21] T. Nishikawa, K. Suzuki, S. Ito, K. Sato, T. Takebe, Decomposition of synthetic ettringite by carbonation, Cement Concrete Res. 22 (1992) 6–14.
[22] M. Kõiv, M. Liira, Ü. Mander, R. Mõtlep, C. Vohla, K. Kirsimäe, Phosphorus removal using Ca-rich hydrated oil shale ash as filter material – the effect of different phosphorus loadings and wastewater compositions, Water Res. (2010), doi:10.1016/j.watres.2010.06.044.
[23] A. Meunier, Clays, Springer, Berlin, Heidelberg, 2005.
[24] O. Hjelmar, Leachate from land disposal of coal fly ash, Waste Manage. Res. 8 (1990) 429–449.
[25] A.G. Kim, The effect of alkalinity of Class F PC fly ash on metal release, Fuel 85 (2006) 1403–1410.
[26] O. Velts, M. Hautaniemi, J. Kallas, M. Kuosa, R. Kuusik, Modeling calcium dissolution from oil shale ash. Part 2. Continuous washing of the ash layer, Fuel Process. Technol. (2010), doi:10.1016/j.fuproc.2009.12.009.